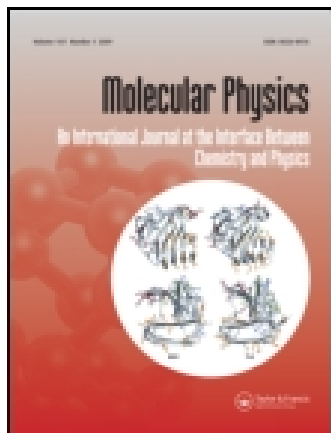


This article was downloaded by: [University of Lethbridge]

On: 28 July 2015, At: 16:50

Publisher: Taylor & Francis

Informa Ltd Registered in England and Wales Registered Number: 1072954 Registered office: 5 Howick Place, London, SW1P 1WG



Molecular Physics: An International Journal at the Interface Between Chemistry and Physics

Publication details, including instructions for authors and subscription information:

<http://www.tandfonline.com/loi/tmph20>

The far-infrared spectrum of $^{12}\text{C}_2\text{HD}$

A. Predoi-Cross^a, M. Herman^b, L. Fusina^c & G. Di Lonardo^c

^a Department of Physics and Astronomy, University of Lethbridge, 4401 University Drive, Lethbridge, AB T1K 3M4, Canada

^b Laboratoire de Chimie quantique et Photophysique, CP160/09, Faculté des Sciences, Université Libre de Bruxelles, 50 Av. Roosevelt, B-1050 Bruxelles, Belgium

^c Dipartimento di Chimica Fisica e Inorganica, Facoltà di Chimica Industriale, Università di Bologna, Viale Risorgimento 4, 40136 Bologna, Italy

Published online: 25 Nov 2010.

To cite this article: A. Predoi-Cross, M. Herman, L. Fusina & G. Di Lonardo (2011) The far-infrared spectrum of $^{12}\text{C}_2\text{HD}$, *Molecular Physics: An International Journal at the Interface Between Chemistry and Physics*, 109:4, 559-563, DOI: [10.1080/00268976.2010.536170](https://doi.org/10.1080/00268976.2010.536170)

To link to this article: <http://dx.doi.org/10.1080/00268976.2010.536170>

PLEASE SCROLL DOWN FOR ARTICLE

Taylor & Francis makes every effort to ensure the accuracy of all the information (the "Content") contained in the publications on our platform. However, Taylor & Francis, our agents, and our licensors make no representations or warranties whatsoever as to the accuracy, completeness, or suitability for any purpose of the Content. Any opinions and views expressed in this publication are the opinions and views of the authors, and are not the views of or endorsed by Taylor & Francis. The accuracy of the Content should not be relied upon and should be independently verified with primary sources of information. Taylor and Francis shall not be liable for any losses, actions, claims, proceedings, demands, costs, expenses, damages, and other liabilities whatsoever or howsoever caused arising directly or indirectly in connection with, in relation to or arising out of the use of the Content.

This article may be used for research, teaching, and private study purposes. Any substantial or systematic reproduction, redistribution, reselling, loan, sub-licensing, systematic supply, or distribution in any form to anyone is expressly forbidden. Terms & Conditions of access and use can be found at <http://www.tandfonline.com/page/terms-and-conditions>

RESEARCH ARTICLE

The far-infrared spectrum of $^{12}\text{C}_2\text{HD}$

A. Predoi-Cross^a, M. Herman^b, L. Fusina^c and G. Di Lonardo^{c*}

^aDepartment of Physics and Astronomy, University of Lethbridge, 4401 University Drive, Lethbridge, AB T1K 3M4, Canada;

^bLaboratoire de Chimie quantique et Photophysique, CP160/09, Faculté des Sciences, Université Libre de Bruxelles, 50 Av. Roosevelt, B-1050 Bruxelles, Belgium; ^cDipartimento di Chimica Fisica e Inorganica, Facoltà di Chimica Industriale, Università di Bologna, Viale Risorgimento 4, 40136 Bologna, Italy

(Received 15 September 2010; final version received 26 October 2010)

The infrared spectrum of $^{12}\text{C}_2\text{HD}$ has been studied using synchrotron radiation at the far-infrared beam line, Canadian Light Source, Saskatoon, Canada. The spectra were recorded at a resolution of 0.00096 cm^{-1} in the 60 to 360 cm^{-1} range using a Bruker IFS 125 Fourier transform spectrometer. In total, 821 vibration rotation lines were observed and assigned to the P(J), Q(J) and R(J) transitions of the $\nu_5 \leftarrow \nu_4$ difference band and associated hot bands with J'' up to 35 and $(\nu_4 + \nu_5)$ up to 3. These new transitions were analysed together with 4518 transitions involving bending states with $(\nu_4 + \nu_5)$ up to 3 available in the literature. The spectroscopic parameters obtained from the fit reproduce 4909 transitions with a standard deviation of 0.00028 cm^{-1} . The $\nu_5 \leftarrow \nu_4$ bands of $^{13}\text{CH}^{12}\text{CD}$ and $^{12}\text{CH}^{13}\text{CD}$ were also detected and analysed.

Keywords: deuterated acetylene; $^{12}\text{C}_2\text{HD}$; FIR spectrum; bendings; high resolution

1. Introduction

Before its detection in the Titan atmosphere by the Composite Infrared Spectrometer (CIRS) instrument mounted on the CASSINI spacecraft [1], mono-deuterated acetylene ($^{12}\text{C}_2\text{HD}$) had never been considered a molecule of astrophysical interest. Prior to this finding, deuterated species of methane and hydrogen had been identified in the atmospheric spectra of Titan, where methane is considered to be the main reservoir of deuterium. The discovery of mono-deuterated acetylene in Titan's atmosphere and inconsistencies in the H/D ratio retrieved from the analysis of different vibrational bands of methane have prompted a thorough investigation of the infrared intensities of $^{12}\text{C}_2\text{HD}$ in the $400\text{--}2000\text{ cm}^{-1}$ range [2], with particular emphasis on the bending fundamentals, the strong features of which could be useful for the evaluation of the H/D ratio in Titan's atmosphere.

Although the spectroscopy of this molecule in the infrared (IR) is very well known [3–9], the only observations reported so far in the far-IR refer to the pure rotational spectrum in the ground and in a few low-lying vibrational states [10–12]. Mono-deuterated acetylene has two doubly degenerate bending vibrations at 518.38 cm^{-1} (ν_4) and 677.86 cm^{-1} (ν_5). The spectral signatures of both these vibrations have been observed in Titan's atmospheric spectra. From a

spectroscopic point of view, it is expected that the difference band $\nu_5 \leftarrow \nu_4$ will appear near 159.48 cm^{-1} , as observed in normal acetylene at 116.28 cm^{-1} [13–16]. In addition, a large number of hot bands accompanying the difference band should appear in the same region. Synchrotron light offers a significant advantage compared with a thermal source over most of the far-infrared region and was adopted as the source in our experiment in order to improve the S/N ratio of the recorded spectra.

2. Experimental details

Two spectra were acquired during separate experiments involving a Bruker IFS 125 Fourier transform (FT) spectrometer located at the far-infrared beam line, Canadian Light Source, Saskatoon, Canada. The spectra were recorded in the $60\text{--}360\text{ cm}^{-1}$ range at an unapodized resolution of 0.00096 cm^{-1} . Optimum instrumental performance was achieved using a synchrotron source, a 2 mm Mylar beam splitter, and a Si bolometer detector. The spectrometer aperture was set to 2 mm. A scanner velocity of 80 kHz was used with analog electronic filters set for a low band pass of 5 kHz. No optical filters were used. A boxcar apodization was used in the Fourier transform, which leads to an instrumental linewidth of 0.61/optical path

*Corresponding author. Email: dilo@ms.fci.unibo.it

difference, full width at half maximum. A zero filling factor of 2, a Mertz phase correction, and a phase resolution of 1.0 were also used in the Fourier transforms.

A multi-pass coolable cell with a base of 2 m with wedged polypropylene windows adjusted for a 72 m path length held the C_2HD sample. The sample was supplied by Cambridge Isotope Laboratories and used without further purification. The isotopic purity was reported to be 98%, but it turned out that C_2H_2 was more abundant than expected. In particular, transitions of the symmetric species interfere with the P branch of the $\nu_5 \leftarrow \nu_4$ band of C_2HD . Nevertheless, due to the very high resolution, the number of overlapping lines is negligible. All far-infrared data for the C_2H_2 isotopologue, recorded under similar experimental conditions, are well known [16] and were easily identified in the spectra.

The two spectra were recorded using the following pressure/temperature conditions: 0.750 Torr/298.35 K (spectrum I) and 3.026 Torr/297.75 K (spectrum II). The gas pressure was measured using a 0–1 Torr and a 0–10 Torr Baratron gauge for spectra I and II, respectively. Rotational water lines [17,18] were used to calibrate the wavenumber scale. Lines of the intense $\nu_5 \leftarrow \nu_4$ band were measured on spectrum I, while lines of all the other hot bands and of $^{13}CH^{12}CD$ and $^{12}CH^{13}CD$ rely on spectrum II.

3. Analysis

The position of the lines expected in the investigated spectral range was calculated by means of the parameters derived from the analysis of the bending states up to $\nu_4 + \nu_5 = 3$ [4]. First, the intense $\nu_5 \leftarrow \nu_4$ band was investigated. The P and R branches could be assigned up to high J values, while the weak Q branch lines were observed up to $J = 13$. Figure 1 illustrates the $f \leftarrow e$ and $e \leftarrow f$ components of the Q branch. Subsequently, a systematic search of the lines belonging to all weak hot bands involving states up to $\nu_{tot} = \nu_4 + \nu_5 = 3$ present in the recorded region was undertaken. All bands involving states with $\nu_{tot} = 2$ were identified, but, within the investigated range, only the P and Q branches of the $2\nu_4 \leftarrow \nu_5$ ($\Sigma^+ \leftarrow \Pi$) band were present, while the expected P lines of the $\Delta \leftarrow \Pi$ component were too weak to be observed. These latter branches are at the upper wavenumber limit of the spectrum, which is characterized by a poor S/N ratio. Of the transitions involving three quanta of the bending modes, only the $\nu_4 + 2\nu_5 \leftarrow 2\nu_4 + \nu_5$ ($\Phi \leftarrow \Phi$) and $2\nu_4 + \nu_5 \leftarrow 3\nu_4$ (${}^1\Pi \leftarrow \Pi$) bands were identified. After completing the assignment procedure, a careful search

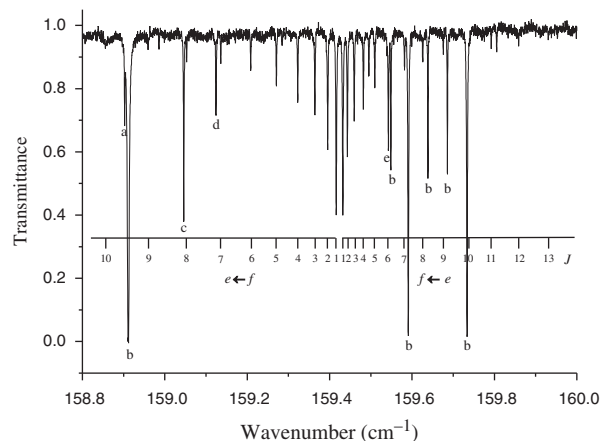


Figure 1. A section of the FIR spectrum illustrating the Q branch of the $\nu_5 \leftarrow \nu_4$ band of $^{12}C_2HD$. Experimental conditions: pressure, 3.026 Torr; path length, 72 m. (a) The $R(15)$ transition of $2\nu_5\Sigma^+ \leftarrow \nu_4 + \nu_5\Sigma^+$ in $^{12}C_2H_2$. (b) The rotational transition in H_2O . (c) The $R(18)$ transition of $(\nu_4 + \nu_5)\Delta_u(e) \leftarrow 2\nu_4\Delta_g(e)$ in $^{12}C_2H_2$. (d) The $10_{4,6} \leftarrow 9_{4,5}$ rotational transition in HOD. (e) The $R(8)$ transition of $2\nu_5\Sigma^+ \leftarrow (\nu_4 + \nu_5)\Sigma^+$ in $^{12}C_2HD$.

for $\Delta(l_4 + l_5) = 2$ transitions was undertaken by means of a list of computed wavenumbers. Three such bands with intensity slightly above the noise level of the spectrum were found with origins at 146.48, 161.78, and 161.81 cm^{-1} . The assignment of the transitions was straightforward due to the accuracy of their predicted positions. The analysed bands are listed in Table 1 together with the symmetry of the vibrational states, the band centre, the J values of the P, Q, and R branches, the RMS value of the residuals obtained from a simultaneous fit, and the number of lines assigned and retained in the final cycle of the least-squares procedure.

After having completed the assignments, a simultaneous fit of all the transitions involving only excited states of the bending modes was performed. The data set includes: (i) the presently observed far-IR transitions, (ii) the IR bands listed in Table 1 of Ref. [4] involving all the states with $\nu_{tot} = 3$, with the exception of the $\nu_4 = 3\Phi$ state which was not observed, (iii) the $2\nu_4 + \nu_5 \leftarrow 2\nu_4$ (${}^1\Pi \leftarrow \Delta$) band reported in Ref. [2] and (iv) the rotational lines in the ground and first excited bending states $\nu_4 = 1$ and $\nu_5 = 1$ [11,12]. The model Hamiltonian adopted for the analysis has already been described (see Ref. [4], Equations (2)–(6)). It contains the usual vibration and rotation terms for a linear molecule with two bending modes, including the l -type interaction terms, both vibrational and rotational, connecting levels of the same vibrational manifold.

Table 1. The bands of $^{12}\text{C}_2\text{HD}$, $^{12}\text{CH}^{13}\text{CD}$ and $^{13}\text{CH}^{12}\text{CD}$ analysed in the far-IR spectrum.

Vibrational transition	Symmetry	$\nu_{\text{C}}^{\text{a}}$	P, R, Q $\{J_{\text{min}}, J_{\text{max}}\}$	$\sigma(\times 10^5)^{\text{b}}$	No. fitted/assigned lines
$^{12}\text{C}_2\text{HD}$					
$\nu_5 \leftarrow \nu_4$	$\Pi \leftarrow \Pi$	159.4263	$\text{P}_{\text{e-e}}(2-33), \text{R}_{\text{e-e}}(1-35),$ $\text{Q}_{\text{f-e}}(1-13); \text{P}_{\text{f-f}}(2-34),$ $\text{R}_{\text{f-f}}(1-35), \text{Q}_{\text{f-e}}(1-12)$	5	152/159
$2\nu_4 \leftarrow \nu_5$	$\Sigma^+ \leftarrow \Pi$	356.1275	$\text{P}_{\text{e-e}}(3-23), \text{Q}_{\text{e-f}}(2-23)$	26	42/43
$\nu_4 + \nu_5 \leftarrow 2\nu_4$	$\Sigma^+ \leftarrow \Sigma^+$	166.5628	$\text{P}_{\text{e-e}}(1-24), \text{R}_{\text{e-e}}(0-28)$	11	53/53
	$(\Sigma^+ \leftarrow \Delta)^{\text{c}}$	161.7773	$\text{P}_{\text{e-e}}(9-28), \text{R}_{\text{e-e}}(8-34)$	20	42/47
	$\Delta \leftarrow \Delta$	157.0286	$\text{P}_{\text{e-e}}(3-24), \text{R}_{\text{e-e}}(2-30),$ $\text{Q}_{\text{e-f}}(2-11); \text{P}_{\text{f-f}}(3-29),$ $\text{R}_{\text{f-f}}(2-33), \text{Q}_{\text{f-e}}(2-14)$	13	129/133
	$(\Delta \leftarrow \Sigma^+)^{\text{c}}$	161.8141	$\text{P}_{\text{e-e}}(9-27), \text{R}_{\text{e-e}}(8-32)$	22	42/44
$2\nu_5 \leftarrow \nu_4 + \nu_5$	$\Sigma^+ \leftarrow \Sigma^+$	141.7283	$\text{P}_{\text{e-e}}(1-20), \text{R}_{\text{e-e}}(1-29)$	10	49/49
	$\Delta \leftarrow \Delta$	163.2996	$\text{P}_{\text{e-e}}(3-26), \text{R}_{\text{e-e}}(2-29),$ $\text{Q}_{\text{e-f}}(2-11); \text{P}_{\text{f-f}}(3-24),$ $\text{R}_{\text{f-f}}(2-30), \text{Q}_{\text{f-e}}(2-12)$	13	119/124
	$(\Sigma^+ \leftarrow \Delta)^{\text{c}}$	146.4771	$\text{P}_{\text{e-e}}(12-19), \text{R}_{\text{e-e}}(15-29)$	14	20/23
$\nu_4 + 2\nu_5 \leftarrow 2\nu_4 + \nu_5$	$\Phi \leftarrow \Phi$	160.9732	$\text{P}_{\text{e-e}}(4-16), \text{R}_{\text{e-e}}(3-22),$ $\text{Q}_{\text{e-f}}(3-8); \text{P}_{\text{f-f}}(5-18),$ $\text{R}_{\text{f-f}}(5-24), \text{Q}_{\text{f-e}}(3-10)$	25	71/77
$2\nu_4 + \nu_5 \leftarrow 3\nu_4$	${}^1\Pi \leftarrow \Pi$	171.3139	$\text{P}_{\text{e-e}}(3-20), \text{R}_{\text{e-e}}(1-19);$ $\text{P}_{\text{f-f}}(3-17), \text{R}_{\text{f-f}}(1-17),$ $\text{Q}_{\text{f-e}}(1)$	22	63/69
$^{12}\text{CH}^{13}\text{CD}$					
$\nu_5 \leftarrow \nu_4$	$\Pi \leftarrow \Pi$	166.3566	$\text{P}_{\text{e-e}}(2-18), \text{R}_{\text{e-e}}(2-23);$ $\text{P}_{\text{f-f}}(3-21), \text{R}_{\text{f-f}}(1-25)$	22	72/81
$^{13}\text{CH}^{12}\text{CD}$					
$\nu_5 \leftarrow \nu_4$	$\Pi \leftarrow \Pi$	157.6795	$\text{P}_{\text{e-e}}(2-19), \text{R}_{\text{e-e}}(1-24);$ $\text{P}_{\text{f-f}}(3-18), \text{R}_{\text{f-f}}(1-24)$	22	76/82

Notes: ${}^{\text{a}}\nu_{\text{C}} = G_{\nu'}^0 - B_{\nu'}k^2 - D_{\nu'}k^4 - (G_{\nu''}^0 - B_{\nu''}k^2 - D_{\nu''}k^4)$.

${}^{\text{b}}\sigma$ (in cm^{-1}) corresponds to the RMS value of the residuals for the various assigned lines resulting from the simultaneous fit (see text).

${}^{\text{c}}$ Perturbation-allowed transition.

The weights of the experimental data were chosen proportional to the inverse of their squared estimated uncertainties. An uncertainty of $5 \times 10^{-5} \text{cm}^{-1}$ (1.66 MHz) was given to wavenumbers of the main band $\nu_5 \leftarrow \nu_4$, $1 \times 10^{-4} \text{cm}^{-1}$ to those of the weak bands involving $\nu_{\text{tot}}=2$, but for $2\nu_4 \leftarrow \nu_5$ ($\Sigma^+ \leftarrow \Pi$), which is at the edge of the response curve of the bolometer, an uncertainty of $2 \times 10^{-4} \text{cm}^{-1}$ was given and to the remaining far-IR transitions with $\nu_{\text{tot}}=3$. The uncertainty of the IR lines was estimated to be $2 \times 10^{-4} \text{cm}^{-1}$, while that of the pure rotational lines was set to $1 \times 10^{-6} \text{cm}^{-1}$ (30 kHz). Finally, all the transition wavenumbers that differed from their corresponding calculated values by more than five times their uncertainties were excluded from the data set in the final cycle of the analysis.

A total of 5339 transitions were fitted to 62 parameters (see Table 2). Based on the criterion adopted for rejection, 4909 observed wavenumbers

were reproduced with a standard deviation of the fit of $2.8 \times 10^{-4} \text{cm}^{-1}$. The RMS error for each band presently analysed is reported in column 5 of Table 1. For the bands previously observed, the RMS errors are practically identical to the values obtained in the fit without the far-IR transitions [4].

The spectroscopic parameters in Table 2 can be compared with those listed in Table 2 of Ref. [4], taking into account that, in the latter table, the parameter q_5^k is erroneously written as q_4^k . The same constants have been refined, but δ_{45} (see Equation (3) of Ref. [4]) remained undetermined and was constrained to zero. The inability to determine δ_{45} could be ascribed to the reduced correlation between the parameters related to the vibrational dependence of the centrifugal distortion constant D_0 resulting from the inclusion of new very precise measurements in the data set. The values of all the parameters are very similar, most being determined within one statistical

Table 2. Spectroscopic parameters (in cm^{-1}) for the bending states of $^{12}\text{C}_2\text{HD}$ resulting from the simultaneous fit of all transitions involving levels up to $\nu_4 + \nu_5 = 3$.^a

Parameter			Parameter		
ω_4^0	517.400373	(268)	g_{55}^0	5.1618252	(245)
ω_5^0	676.1870743	(371)	γ_4^{44}	0.037851	(105)
x_{44}^0	-0.143558	(197)	γ_4^{45}	-0.1020412	(223)
x_{45}^0	0.7075504	(548)	γ_4^{55}	0.0218842	(201)
x_{55}^0	-2.5974508	(266)	γ_3^{44}	0.0398552	(309)
y_{444}^0	-0.0364024	(323)	γ_5^{45}	-0.0497324	(186)
y_{555}^0	0.03026340	(611)	γ_5^{55}	0.01895520	(936)
y_{455}^0	0.0426422	(187)	r_{45}^0	1.557113	(195)
y_{445}^0	0.0427599	(215)	r_{445}	0.2380359	(560)
g_{44}^0	2.117292	(210)	r_{455}	0.067199	(103)
g_{45}^0	0.8521726	(394)	$r_{45}^J (\times 10^3)$	-0.0246653	(746)
B_0	0.9915272623	(434)	$\gamma_{445} (\times 10^6)$	2.0464	(460)
$\alpha_4^0 (\times 10^3)$	-2.643371	(138)	$\gamma_{455} (\times 10^6)$	0.2716	(367)
$\alpha_5^0 (\times 10^3)$	-1.481912	(103)	$\gamma_4^{44} (\times 10^6)$	-1.1851	(675)
$\gamma_{44} (\times 10^3)$	0.0313649	(561)	$\gamma_4^{45} (\times 10^6)$	2.2258	(709)
$\gamma_{45} (\times 10^3)$	-0.025949	(109)	$\gamma_4^{55} (\times 10^6)$	-0.3491	(279)
$\gamma_{55} (\times 10^3)$	0.0236638	(383)	$\gamma_5^{44} (\times 10^6)$	-2.1443	(526)
$\gamma^{44} (\times 10^3)$	-0.079675	(145)	$\gamma_3^{45} (\times 10^6)$	2.9576	(513)
$\gamma^{45} (\times 10^3)$	-0.003360	(151)	$\gamma_5^{55} (\times 10^6)$	-2.3959	(331)
$\gamma^{55} (\times 10^3)$	-0.1187171	(855)			
$D_0 (\times 10^6)$	1.133919	(183)	$\delta_{55} (\times 10^9)$	0.2737	(194)
$\beta_4 (\times 10^6)$	0.0345719	(927)	$\delta^{44} (\times 10^9)$	2.1478	(575)
$\beta_5 (\times 10^6)$	0.0167646	(773)	$\delta^{55} (\times 10^9)$	-2.0065	(302)
$\delta_{44} (\times 10^9)$	-0.9328	(301)			
$H_0 (\times 10^{12})$	0.5733	(943)	$h_5 (\times 10^{12})$	0.1947	(237)
$h_4 (\times 10^{12})$	0.2021	(330)			
$q_4^0 (\times 10^3)$	4.3977317	(637)	$q_{55} (\times 10^3)$	0.0478092	(274)
$q_5^0 (\times 10^3)$	3.4783596	(639)	$q_4^J (\times 10^6)$	-0.0383910	(394)
$q_{44} (\times 10^3)$	0.0406380	(394)	$q_5^J (\times 10^6)$	-0.0221680	(437)
$q_{45} (\times 10^3)$	-0.0054381	(415)	$q_5^k (\times 10^6)$	-5.0948	(789)
$q_{54} (\times 10^3)$	0.0178707	(718)			
$\rho_4^0 (\times 10^6)$	-0.011018	(114)	$\rho_{55} (\times 10^9)$	5.490	(208)
$\rho_5^0 (\times 10^6)$	-0.012120	(447)	$\rho_{45}^0 (\times 10^9)$	-0.868	(258)

Notes: Number of fitted/assigned data: 4909/5339. St. dev. of the fit $\times 10^4 = 2.8$.

^aEstimated uncertainties (1σ) are given in parentheses in units of the last figure quoted.

error. Those presently obtained have smaller uncertainties, on average about 20%, due to the high precision of the far-IR data and to the extension of pure rotational transitions measured with higher accuracy up to $J=10$ [12].

Finally, transitions of the $\nu_5 \leftarrow \nu_4$ bands of $^{13}\text{CH}^{12}\text{CD}$ and $^{12}\text{CH}^{13}\text{CD}$ were identified and analysed in single-band fits. The band characteristics are listed in Table 1. A table with a list of the transition wavenumbers, assignments, and residuals

from the simultaneous fit associated with all the analysed bands can be made available from the Bologna authors.

4. Conclusions

The very high resolution far-IR spectrum of mono-deuterated acetylene, $^{12}\text{C}_2\text{HD}$, has been recorded in the 60–360 cm^{-1} region using FT spectroscopy and a synchrotron radiation source. The

analysis of the observed bands complements and improves previous investigations on the bending states of the molecule. A simultaneous fit of 5339 transitions, including all previously measured lines and those presently assigned, provides a set of 62 accurate spectroscopic parameters that reproduces 4909 transitions with a standard deviation of the fit of $2.8 \times 10^{-4} \text{ cm}^{-1}$.

Acknowledgements

All authors are indebted to Mr. Brant Billingham for recording the spectra. G. Di Lonardo and L. Fusina thank the University of Bologna and the MIUR (PRIN Trasferimento di energia e di carica: dalle collisioni ai processi dissipativi). M. Herman thanks the Fonds National de la Recherche Scientifique (F.R.S.-FNRS, contracts FRFC and IISN) and the 'Action de Recherches Concertées de la Communauté française de Belgique'. A. Predoi-Cross is grateful for research support provided by the Natural Sciences and Engineering Research Council of Canada.

References

- [1] A. Coustenis, D.J. Jennings, A. Jolly, Y. Benilan, C.A. Nixon, S. Vinatier, D. Gautier, G.L. Bjoraker, P.N. Romani, R.C. Carlson and F.M. Flasar, *Icarus* **197**, 539 (2008).
- [2] A. Jolly, Y. Benilan, E. Canè, L. Fusina, F. Tamassia, A. Fayt, S. Robert and M. Herman, *J. Quant. Spectrosc. Radiat. Transf.* **109**, 2846 (2008).
- [3] A. Baldacci, S. Gheretti, S.C. Hurlock and K. Narahari Rao, *J. Mol. Spectrosc.* **59**, 116 (1976).
- [4] L. Fusina, E. Canè, F. Tamassia and G. Di Lonardo, *Mol. Phys.* **103**, 3263 (2005).
- [5] L. Fusina, F. Tamassia and G. Di Lonardo, *Mol. Phys.* **103**, 2613 (2005).
- [6] J. Liévin, M. Abouti Tamsamani, P. Gaspard and M. Herman, *Chem. Phys.* **190**, 419 (1995).
- [7] M. Abouti Tamsamani and M. Herman, *Chem. Phys. Lett.* **260**, 253 (1996).
- [8] M. Abouti Tamsamani and M. Herman, *Chem. Phys. Lett.* **264**, 556 (1997).
- [9] M. Herman, C. Depiesse, G. Di Lonardo, A. Fayt, L. Fusina, D. Hurtmans, S. Kassi, M. Mollabashi and J. Vander Awera, *J. Mol. Spectrosc.* **228**, 499 (2004).
- [10] K. Matsumura, T. Tanaka, Y. Endo, S. Saito and E. Hirota, *J. Phys. Chem.* **84**, 1793 (1980).
- [11] G. Wlodarczak, J. Demaison, J. Burie and M.C. Lasne, *Mol. Phys.* **66**, 669 (1989).
- [12] G. Cazzoli, C. Puzzarini, L. Fusina and F. Tamassia, *J. Mol. Spectrosc.* **247**, 115 (2008).
- [13] Y. Kabbadj, M. Herman, G. Di Lonardo, L. Fusina and J.W.C. Johns, *J. Mol. Spectrosc.* **150**, 535 (1991).
- [14] D. Jacquemart, L. Gomez, N. Lacome, J.-Y. Mandin, O. Pirali and P. Roy, *J. Quant. Spectrosc. Radiat. Transf.* **110**, 2102 (2009).
- [15] S. Yu, B.J. Drouin and J.C. Pearson, *Astrophys. J.* **705**, 786 (2009).
- [16] B. Amyay, M. Herman, A. Fayt, L. Fusina and A. Predoi-Cross, *Chem. Phys. Lett.* **491**, 17 (2010).
- [17] J.W.C. Johns, *J. Opt. Soc. Am. B* **2**, 1340 (1985).
- [18] F. Matsushima, H. Odashima, T. Iwasaki, S. Tsunekawa and K. Takagi, *J. Mol. Struct.* **352/353**, 371 (1995).